The 6th International Conference on
Structural Health Monitoring of Intelligent Infrastructure
Hong Kong | 9-11 December 2013

SYSTEM IDENTIFICATION OF SHEAR-DEFORMATION BUILDINGS WITH CONTINUOUS-DISCRETE MODELING

R.C. Zhang
Department of Civil and Environmental Engineering, Colorado School of Mines, Golden, Colorado, USA.
Email: rzhang@mines.edu

ABSTRACT

This study presents a continuous-discrete model for seismic shear motion in multi-story buildings and shows their applications in inverse parametric identification. In particular, the building is modeled as a series of shear-beams for inter-story columns/walls and lumped-masses for rigid floors. Shear motion response at one location of the building is then obtainable to an impulsive motion at another location in the time and frequency domains, termed here as generalized impulse and frequency response functions (GIRF and GFRF). The GIRF and GFRF are not only fundamental in relating seismic responses at the two locations of a building structure subjected to ground seismic excitation that is not fully known due to the complicated soil-structure interaction. They also play a key role in characterizing structural responses, as well as in identifying dynamic parameters of the building. For illustration, this study examines response features of ten-story building of Millikan Library in Pasadena, California with the Yorba Linda earthquake of September 3, 2002. With the use of the continuous-discrete model as well as its degenerated ones, structural responses are interpreted from the perspective of wave propagation, and more importantly validated with the pertinent recordings and discrete-model-based results. Parametric identification of the building with a pair of seismic recordings is then presented. This study concludes that the proposed approach is efficient and robust in comparison with the traditional discrete-based ones in forward predicting analysis and inverse system identification.

KEYWORDS

Continuous-discrete modeling, seismic structural responses, shear wave motion, system identification.

INTRODUCTION

For seismic design, vibration control, and damage diagnosis of multi-story buildings such as ten-story Millikan Library in Figure 1, response characterization and system identification are fundamental and typically carried out with an MDOF model. As far as 1D horizontal motion is concerned for example, the Millikan Library building can be modeled as a 10-DOF system with each floor mass and inter-story stiffness (i.e., physical parameters) calculable based on design configuration and materials. These physical parameters can also be calibrated in terms of identified vibratory features (i.e., modal frequencies and shapes—a function of physical parameters), through Fourier spectral analysis of 11-set acceleration recordings of the Yorba Linda earthquake of September 3, 2002 in Figure 2. Subsequently, seismic demand such as structural peak acceleration to a scenario earthquake is predictable, which is useful for seismic design/retrofit and vibration control. Similarly, change of some physical parameters or high-order modal parameters are identifiable with 11-set recordings of a new earthquake, which is detection and quantification of local, minor damage in post-earthquake structural condition evaluation. Furthermore, implementing damage mechanism such as material hysteresis, plastic hinge, and/or crack into the linear 10-DOF model

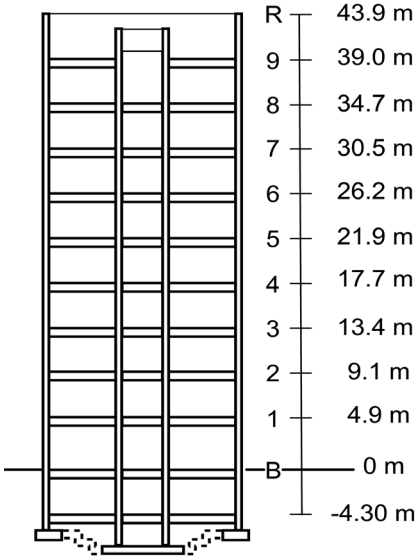

Figure 1. Vertical cross-section of 10-story Millikan Library, Pasadena, California

would make the modeling rigorous in simulating nonlinear vibratory features, thus enhancing credibility in forward predicting analysis and inverse system identification, among many other broad-based applications (Xu et al. 2003; Hong et al. 2009; Benejree 2009 and Uluso et al. 2011).

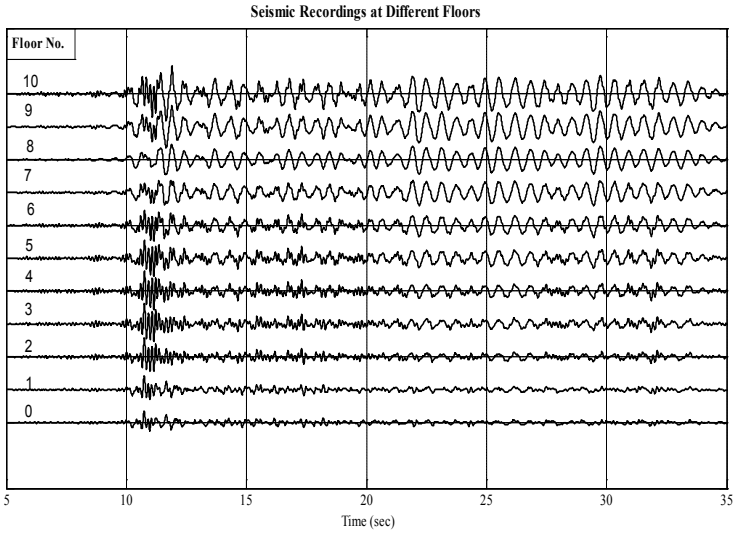

Figure 2. Seismic acceleration recordings of the Yorba Linda earthquake in the North-South direction at different floors (indicated as 0~10), where floor levels 0 and 10 correspond to *B* and *R*, respectively, in Figure 1

While the aforementioned discrete modeling is overwhelmingly used in structural engineering (Chopra 1995; Lin and Cai 1995), it has limitation in efficiently characterizing comprehensive seismic motion in structures with *finite*-DOF modeling in general, and distorting time-space representation of seismic motion in buildings in particular. For illustration, seismic responses synthesized with the 10-DOF model will overlook the authentic floor-to-floor propagation features of high-frequency, dominant-energy waves, observed prominently in the 10~12s time window in Figure 2.

In fact, seismic responses are the result of wave propagation in large-scale structures such as high-rise buildings, in which some wave-propagation features, exemplified as flight time of waves traveling from one location to the other, play an important role in in-depth understanding of seismic recordings and effective identification of local structural features. Indeed, recent studies show advantages of continuous-modeling over traditional discrete-modeling in some seismic response analyses and system identification and/or damage diagnosis of building structures. For example, Iwan (1996) proposed to use 1D uniform shear-beam model for buildings and obtained seismic drift spectrum for design. Safak (1999) introduced 1D continuous/discrete modeling for structure-soil system with impulsive seismic excitation in bedrock. With the model, he solved for wave responses *numerically* with time-domain analysis methodology, compared them with MDOF structural modeling with ground excitation, and revealed wave-propagation features and influences of soil-structure interaction in seismic structural responses, among others. Todorovska et al. (2001) modeled 2D anisotropic wave propagation for a real seven-story building. While developed over the past decade for exploration seismology, ultrasound and hazard studies, seismic interferometry (SI) was employed (Snider and Safak 2006; Snider et al. 2006) to extract structural responses from seismic recordings. This SI methodology was not only used well for explaining wave phenomena in buildings, but also easily for system identification with a 1D uniform shear-beam model. Subsequently, Kohler et al. (2007) studied seismic propagating waves in a 3D steel moment-frame building and verified with ETABS finite-element modeling, among others (Todorovska et al. 2009a and 2009b). Building upon the aforementioned advances and others in relevant literature (e.g. Lin and Wu 1984; Cai and Lin 1991; Zhang 2000; Kawakami and Oyunchimeg 2003 and 2004; Oyunchimeg and Kawakami 2003; Beyen 2008), Zhang et al. (2010 and 2011) proposed continuous-discrete modeling for 1D wave propagation in building structures, and obtained closed-form solution for seismic response in frequency domain and numerical one in time domain with fast Fourier transform.

This study presents fundamental response features of seismic shear motion in multi-story buildings with the continuous-discrete model and its degenerated ones, and shows their applications in inverse parametric identification with a pair of available recordings.

REVIEW OF CONTINUOUS-DISCRETE MODELING

For convenience in subsequent study, presented below is a brief review for modeling of seismic shear motion in a multi-story building and its closed-form solution for seismic responses (Zhang et al. 2010 and 2011). Figure 3 shows the model consisting of a series of shear-beam layers for inter-story columns/walls and lumped-masses for rigid floors. The j^{th} inter-story layer is characterized by equivalent shear modulus G_j, mass density ρ_j, and

hysteretic damping ratio γ_j, which gives shear wave speed $v_j = \sqrt{G_j/\rho_j}(1 + i\gamma_j \,\mathrm{sgn}(\omega))$ where *sgn(ω)* is the sign of frequency ω and i the imaginary unit. Similarly, the j^{th} floor is described by lumped mass m_{f_j} and viscous damping coefficient of the floor $c_{f_j} = \gamma_{f_j} m_{f_j}$. Seismic wave response of shear displacement *u(z,t)* can then be obtained below by solving force-free wave equation of $\partial^2 u(z,t)/\partial z^2 = v_j^{-2}\partial^2 u(z,t)/\partial t^2$ for each and every inter-stories, together with displacement continuity ($u(z_j,t) = u(z_j^-,t)$ where superscript $^-$ indicates the negative side of height z_j), force dynamic balance at the j^{th} floor (as seen in Figure 3b), and boundary condition at the free top surface (Zhang et al., 2010, 2011; Gargabe, 2012),

$$u(z,t) = \int_{-\infty}^{\infty} D_{Rr}(\omega) U_r(\omega) e^{i\omega t} d\omega = \int_{-\infty}^{\infty} d_{Rr}(t-\tau) u(z_r,\tau) d\tau \tag{1}$$

where $D_{Rr}=U_R/U_r$ and d_{Rr}, referred here to as generalized frequency and impulse response functions (GFRF and GIRF), are respectively displacement responses at response height z (or $z_R=z-z_r$) to an impulsive displacement at reference height z_r in frequency and time domains, and $U_r(\omega) \equiv U(z_r,\omega)$ is the frequency counterpart of $u(z_r,t)$ in which $\equiv$ denotes by definition. A closed-form solution for GFRF, and subsequent GIRF with Fourier transformation of GFRF, can be found as

$$D_{Rr}(\omega) = \frac{(1+R_{NR})T_{Rr}}{(1-R_{rR}R_{NR})(1+R_{Nr})}$$

$$d_{Rr}(t) = \int_{-\infty}^{\infty} D_{Rr} e^{i\omega t} d\omega \tag{2a,b}$$

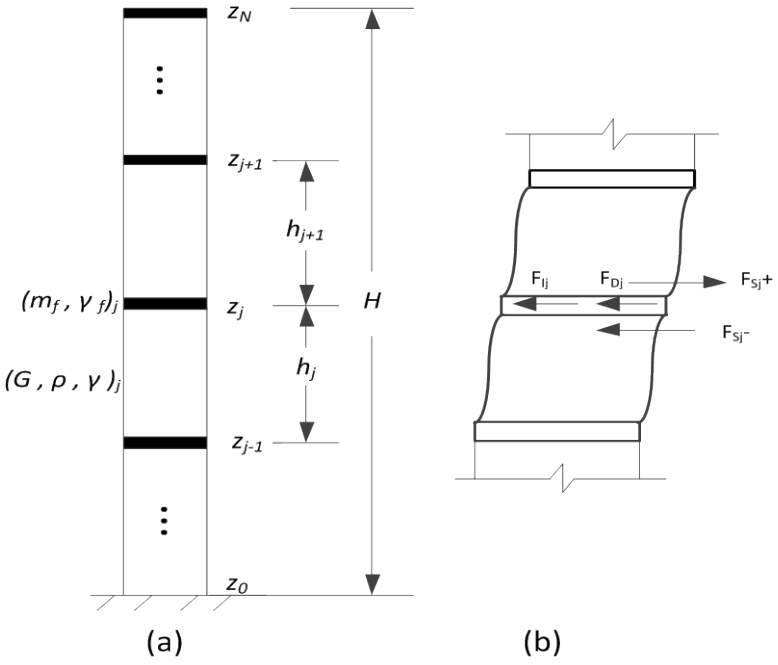

Figure 3. Modeling of *N*-story building: (a) geometrical configuration; (b) deformed shape and forces at selected portion

where wave transmission coefficient T_{Rr} means the up-going wave amplitude at z (or z_R) which is propagated upward from an impulsive up-going wave input at z_r (i.e., $\delta(t)$ in time domain and unit in frequency domain), and reflection coefficient R_{Nr} (similar to other *R*s) is down-going wave amplitude at z_r resulted from an impulsive up-going wave input at z_r which travels upward first, reflects at free top of the N^{th} floor, and then propagates downward to z_r. Expressions of *T*s and *R*s can be found as function of building parameters above z_r. In particular, for the j^{th} inter-story bounded with (z_{j-1},z_j^-)

$$T_{j^-(j-1)} \equiv T_{z_j^- z_{j-1}} = e^{-i\omega h_j/v_j} = T_{(j-1)j^-}, \quad R_{j^-(j-1)} = R_{(j-1)j^-} = 0 \tag{3a}$$

For the j^{th} floor bounded with (z_j^-,z_j)

$$T_{jj^-} = 2/[1 + r_{I_j} - r_{D_j} + i r_{M_j}] = B_{f_j} e^{-i\omega h_{ej}/v_j}, \quad R_{jj^-} = T_{jj^-} - 1, \quad T_{j^-j} = T_{jj^-} r_{I_j}, \quad R_{j^-j} = T_{j^-j} - 1 \tag{3b}$$

where coefficients r_{Ij}, r_{Dj} and r_{Mj}, amplitude B_{fj} and equivalent inter-story height h_{ej} can be found in terms of inter-story impedance (ρv) ratio, cross-sectional area (A) ratio, floor-to-story mass ratio (r_m), wave flight time through inter-story length (h/v), i.e.,

$$\begin{aligned} &r_{I_j} = (\rho_{j+1} v_{j+1} A_{j+1})/(\rho_j v_j A_j), \quad r_{D_j} = \gamma_{f_j} r_{M_j}, \quad r_{M_j} = r_{m_j}\omega(h_j/v_j), \quad r_{m_j} = m_{f_j}/m_j \\ &B_{f_j} = 2[(1 + r_{I_j} - r_{D_j})^2 + r_{M_j}^2]^{-1/2}, \quad h_{ej} = v_j/\omega \tan^{-1}[r_{M_j}/1 + r_{I_j} - r_{D_j}] \end{aligned} \tag{4}$$

For a composite building segment bounded with (z_l,z_n), or simply (l,n), with intermediate location z_m (i.e., $z_l<z_m<z_n$ or $z_l>z_m>z_n$) such as (z_{j-1},z_j) with z_j^-, *T* and *R* between (l,n) can be found in terms of those in two sub-segments of (l,m) and (m,n) as

$$T_{ln} = \frac{T_{lm}T_{mn}}{1 - R_{nm}R_{lm}}, \qquad R_{ln} = R_{mn} + \frac{T_{nm}R_{lm}T_{mn}}{1 - R_{nm}R_{lm}} \tag{5}$$

FUNDAMNETAL RESPONSE FEATURES

This section examines fundamental response features with selected models degenerated from the continuous-discrete one, which could aid in in-depth understanding of the general continuous-discrete model and subsequent applications in system identification.

Model with Two-Layer Media

While a uniform shear-beam model captures fundamental response features of a multi-story building which was also examined in Iwan (1996), Snieder and Safak (2006), Snieder et al. (2006), Zhang et al. (2010 and 2011) and Gargab (2012), piecewise-uniform shear beams would be natural in characterizing changing-properties of the structure along height. For simplicity, one can first examine a two-layer model without floor masses (i.e., inter-stories and floors are treated as equivalent continuous layers), which leads Eq. 2a to the closed form below (see Gargab, 2012)

$$D_{R0} = \frac{\left(1 + \alpha\left(e^{-2i\omega(\tau_1 - \tau_z)} + e^{-2i\omega\tau_2}\right)e^{-2i\omega(\tau - \tau_z)}\right)e^{-i\omega\tau_z}}{1 + \alpha\left(e^{-2i\omega\tau_1} + e^{-2i\omega\tau_2}\right) + e^{-2i\omega\tau}}, \quad 0 \le z \le h_1, \quad \tau_z = \frac{z}{v_1} \tag{6a}$$

$$D_{R0} = \frac{2\left(1 + e^{-2i\omega(\tau - \tau_z)}\right)e^{-i\omega\tau_z} \Big/ \left(1 + r_{I_1}\right)}{1 + \alpha\left(e^{-2i\omega\tau_1} + e^{-2i\omega\tau_2}\right) + e^{-2i\omega\tau}}, \; h_1 \le z \le h_1 + h_2, \; \tau_z = \frac{h_1}{v_1} + \frac{z - h_1}{v_2} \tag{6b}$$

where τ_z is the flight time for waves traveling from referenced level z_r=z_0=0 to response location z_R=z, and

$$\alpha = (1 - r_{I_1})/(1 + r_{I_1}) -, \; \tau_1 = h_1 / v_1, \; \tau_2 = h_2 / v_2, \; \tau = \tau_1 + \tau_2 \tag{7}$$

The GIRF can be found by substituting GFRF of Eqs. 6a,b into Eq. 2b, where solution for the integration can be obtained in a closed form with the method of residues for some special cases and numerically for general cases. Below are presented some special cases, which could help understand the characteristics of wave propagation in piecewise-uniform buildings and subsequently aid in system identification to be elaborated later.

The denominator of Eqs. 6a,b has an infinite number of poles y_j *(j=1,2,..)* in the upper half complex plane, namely

$$1 + \alpha\left(e^{-2iy\tau_1} + e^{-2iy\tau_2}\right) + e^{-2iy\tau} = 0 \;\Rightarrow y_j = \left(\pm 1 + i\gamma_{eq}\right)\omega_j, \; j = 1,2...,\infty \tag{8}$$

For γ_1= γ_2 and τ_1= τ_2, one can find

$$\omega_{2j-1} = [(2j-1)\pi - \beta]/|\tau|, \; \omega_{2j} = [(2j-1)\pi + \beta]/|\tau|, \quad \gamma_{eq} = \gamma_1 = \gamma_2, \quad \alpha = \pm\cos\beta \tag{9}$$

where $|\tau|$ indicates the absolute value of flight time τ. The closed-form solution of GIRF with Eq. 2b for $r_{I_1} = 1$, which could be, but not necessarily, the uniform or one-layer model, can be found as

$$d_{Rr} = [4\pi/|\tau|]\sum_{j=1}^{\infty}(-1)^{j+1} e^{-\gamma\omega_j\left(t - |\tau_z|\right)} \cos\left[\omega_j\left(|\tau| - |\tau_z|\right)\right]\sin\left(\omega_j t\right) \tag{10}$$

Equation 10 indicates that GIRF consists of an infinite number of motion modes, each of which has exponentially decaying damping factor, modal shape with cosine factor, and sinusoidal motion with modal frequency ω_j. This is essentially traditional vibration perspective for structural response, in which the 1st modal frequency ω_1 (similar to high-order modal frequencies) is interpreted as fundamental vibration feature of building's periodic, horizontal motion. Since ω_1 corresponds to fundamental period $T_1 = 4|\tau|$ obtainable from Eq. 9, the fundamental period can also be viewed as four times of wave flight time through the building height, i.e., wave interpretation. All the aforementioned wave-propagation features with the two-layer model are similar to those observed in the uniform shear-beam model (Snieder and Safak 2006; Snieder et al. 2006; Zhang et al. 2010 and 2011).

It is of interest to note that the response features exposed in Eq. 10 with the 2-layer model can also be revealed with traditional *M*DOF models where *M* is typically a large number. This suggests that the former 2-layer model is efficient in capturing response features in comparison with the latter MDOF one. With the same amount of system parameters under consideration, the 2-layer model with six parameters (i.e., two sets of wave velocity, damping and mass density) is also apparently superior to the corresponding 2DOF model with two sets

of stiffness, damping and mass in terms of comprehensive modeling of shear motion in the building. This is even more important from the perspective of effective system identification with a limited number of recordings at hand, which is to be addressed later.

Model with Multiple Continuous-Discrete System

With the understanding of degenerated models and their response features, this sub-section examines wave-propagation features of GIRF with multiple continuous-layers and multiple discrete-masses or simply a multiple continuous-discrete model. Figure 4 shows GIRFs at selected locations with the building modeled as a 11 continuous layers for inter-stories and 11 discrete masses for floors, where all the parameters are shown in case 2 of Table 1. In general, wave features shown in Figure 4 bear the similarity with those with uniform shear-beam model in Zhang et al. (2010, 2011). Specifically, the impulse at the basement (or simply the motion peak at t=0 for convenience) is propagated upward to the 2nd, 4th, 7th and 9th floors with sequential wave-propagation time delay and damping-related amplitude reduction. After hitting the top surface, the positive motion peak is reflected completely without changing motion direction due to the reflection feature at free top (R_{NN}=1, N=11). The time delay of the waves travelling upward from the 9th floor to the top and then downward to the 9th floor generates the second dominant motion peak at the 9th floor, although it is not as clearly seen in Figure 4 as in uniform-beam case in Zhang et al. (2010, 2011). The 2nd peak is then propagated downward to the 7th, 4th and 2nd floors (notably observed at 4th and 2nd floors in Figure 4) and finally disappeared at the basement due to its fixed boundary condition. When the 2nd peak reaches the basement, another up-going wave will be generated with the same-amplitude but opposite motion direction, making the basement motionless at that time instant. This phenomenon can also be explained with transmission and reflection coefficients at the basement ($T_{0\text{-}0}$=0 and $R_{0\text{-}0}$=-1), which indicates down-going wave is completely reflected to the up-going wave with the changed motion direction, and no transmission to the lower end, i.e., fixed basement boundary. The aforementioned cycle of wave propagation continues as time goes on. For earlier time (0-1 s), the GIRF consists primarily of superposition of up-going and down-going travelling shear waves. For later time (>1 s) as the travelling waves can be regarded as standing waves, the GIRF develops the dynamic features characterized by modal frequencies (primarily by the 1st mode or the building resonance), with the amplitude reduced as time goes on (e.g., see GIRF at the 4th floor), which is typically the free-vibration or impulse response phenomenon. The increased amplitude of the GIRFs at the fundamental modal frequency with the position changed from the 2nd to 9th floor is attributed to the wave phenomena with the fixed bottom and free top boundaries.

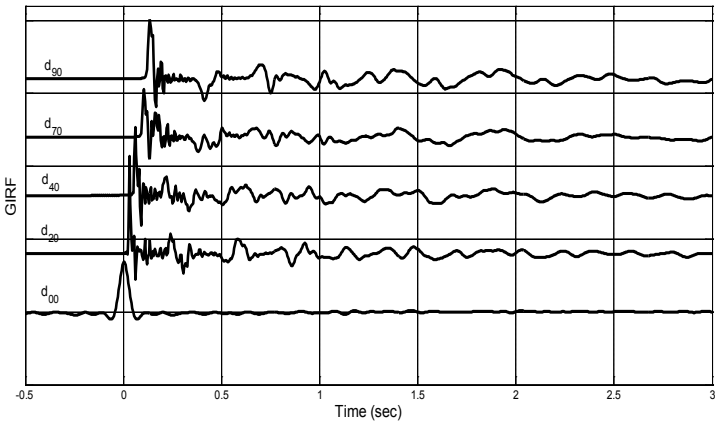

Figure 4. GIRFs at selected floors with continuous-discrete model (the system parameters are shown in case 2 of Table 1)

Besides the aforementioned fundamental wave features, multiple higher-frequency waves are also observed at those presented floors after the first motion peaks in Figure 4. That is primarily caused by wave scattering at each and every of 10 floor-to-story connections, characterized with transmission and reflection coefficients in Eq. 3b. In other words, besides the dominant motion peaks at one floor (say the 1st and 2nd dominant peaks at around 0.1 and 0.25 s for the GIRF at the 4th floor), other multiple peaks after the 1st peak are attributed to the arrival waves reflected and transmitted from other floors (other than the 4th floor). All these make the wave responses complicated after initial arrival of impulsive waves.

The aforementioned response analysis suggests that any change of structural configuration and/or local damage in inter-stories/floors is exposable through the high-frequency wave arrival time among others, which could be useful in system identification and/or damage detection (see Gargab 2012).

SYSTEM IDENTIFICATION OF THE MILLIKAN LIBRARY BUILDING

With advances in understanding forward response features, this section shows inverse system identification of the Millikan Library in California with the use of the general and degenerated shear-deformation building models and a limited number of seismic recordings after the Yorba Linda earthquake of September 3, 2002.

In general, with a pair of seismic recordings at two locations, GFRF is obtainable as Fourier spectral ratio of the two recordings. One can first calculate the recording-based GFRF as

$$\widetilde{D}_{j0} = \frac{\widetilde{U}_j \widetilde{U}_0^*}{|\widetilde{U}_0|^2 + \varepsilon} \xrightarrow{\varepsilon \to 0} \frac{\widetilde{U}_j}{\widetilde{U}_0} \tag{20}$$

where $\widetilde{U}$ is the seismic recording in frequency domain, superscript asterisk indicates the complex conjugate, and ε is a positive small number, implying the added white noise. The white noise is used primarily to avoid unstable calculation of GFRF at some frequencies near the notches in the spectrum $|\widetilde{U}_0|^2$. As ε approaches zero, $\widetilde{D}_{j0}(\omega) \Rightarrow \widetilde{U}_j / \widetilde{U}_0$, which is the Fourier spectral ratio or the definition of GFRF in Eq. 2a. Note that the tilde over quantities *D* and *U* is used to distinguish the recording-based quantities from those derived from the modeling or Eq. 2a.

With the continuous-discrete modeling for building structures, model-based GFRF can also be found in terms of wave transmission and reflection coefficients, which are related to structural physical properties above the impulse location. Matching the two sets of GFRF from recordings and the model helps identify structural parameters such as wave velocity and/or shear modulus.

Parametric Identification with Two-Layer Model

For a pair of recordings available at the basement (i.e., floor 0) and floor 7, GFRF $\widetilde{D}_{70}$, with $\varepsilon = 5\%$ of the total power spectrum of basement motion can be found in Figure 5. In principal, all the frequencies corresponding to the spectral peaks in Figure 5 can be regarded as modal frequencies and then used for system identification. For simplicity and also for illustration with the use of a 2-layer model, parametric identification is carried out here based on two modal frequencies identified from Figure 5 as ω_1=10.62 and ω_2=14.21 *rad/s*.

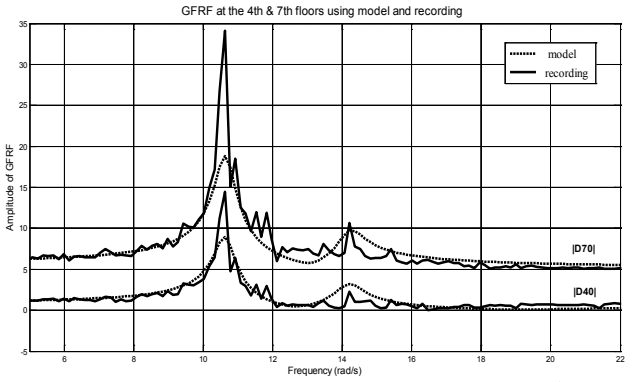

Figure 5. Comparison of GFRF amplitudes at the *4th* and *7th* floors with respect to impulsive basement motion obtained from seismic recordings at the basement, 4th and 7th floors and model

With the use of Eq. 9 and the assumption of the same material without damping and the same cross-sectional area used in both layers, the following two parameters are found

$$|\tau| = \frac{2\pi}{\omega_1 + \omega_2}, \quad \beta = \frac{\pi(\omega_1 + \omega_2)}{\omega_1 + \omega_2} \tag{21}$$

which yields $|\tau|$=*0.253 s* and β=*0.454 rad*, and subsequently r_{I1}=*0.053*, v_1=*361.85 m/s*, v_2=*19.18 m/s*, h_1=*45.77 m*, h_2=*2.43 m* with the aid of Eqs. 4, 7 and 9. The identified slower velocity in thinner layer 2 than those in layer 1 makes sense, for the real building in Figure 1 can be treated as one big portion for layer 1 that consists of 10 rigid floors (from basement to the 9th floor) with large masses and 10 inter-stories with rigid columns and walls, which is below the very thin roof top, the other small portion for layer 2. It should be noted that the

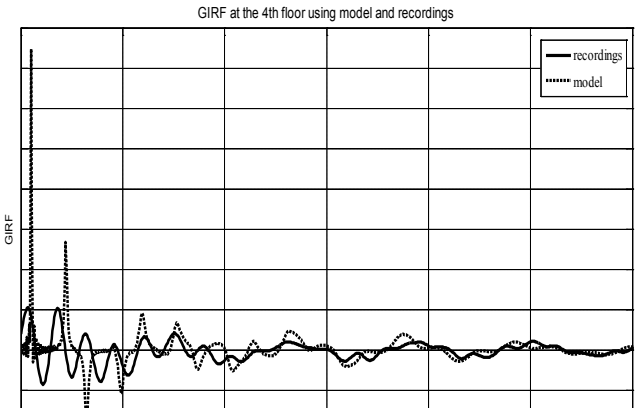

Figure 6. Comparison of GIRF at the 4th floors with respect to basement motion obtained from seismic recordings and model

aforementioned identification is under special condition of $\gamma_1 = \gamma_2 = 0$ and $\tau_1 = \tau_2$, which is apparently not optimized. In general, optimal parameters r_{I1}, v_1, v_2, h_1 and h_2, together with γ_1 and γ_2, can be found by minimizing the mean-square error of the model-based GFRF from recording-based GFRF in certain frequency range (say 5~22 *rad/s*) with the use of certain identification algorithm, among others. While it is doable, this study instead presents the comparison of model-based GFRFs with the aforementioned, identified parameters and $\gamma_1 = \gamma_2 = 0.03$ with recording-based ones, aiming to show the influences of some parameters in GFRF and GIRF. Figures 5 and 6 show respectively the comparison of recording-based GFRF and GIRF at the 4th and 7th floors with respect to white-noise-added ($\varepsilon = 5\%$, see Eq. 20) impulsive motion at the basement against model-based counterparts with respect to pure ($\varepsilon = 0\%$) impulsive motion at basement.

These two figures indicate that the 2-layer model is able to capture fundamental wave and vibration features shown in the recordings, exemplified as the first and second modal frequencies in Figure 5, and proximity of first couples of arrival wave times and well-matched resonant vibration features in Figure 6. The major difference in spectral amplitudes at the first modal frequency in Figure 5 and in wave amplitude and arrival time in the 0~0.5 *s* time window in Figure 6 can be minimized with appropriate system-identification algorithm for identifying layer damping and ε. It is of interest to note that for the same GFRF/GIRF-based system identification with the same pair of recordings in the aforementioned case study, MDOF system in general, and 10- or 2-DOF one in particular, cannot provide as precise building parameters as the 2-layer continuous model, for the former involves either much more parameters with the 10-DOF system or much less DOF in comprehensively modeling the motion than the latter, thus making inverse system identification unreliable. In this sense, the continuous model shows more effectiveness than the traditional discrete, MDOF ones.

Influences of Multiple Layers in Parametric Identification

While some fundamental characteristics of wave-based system identification are shown with a 2-layer model, increased number of layers in the model would be in principle even appropriate in realistically capturing physical multi-story structure of the building.

To see the influence of multi-layer model in system identification, one can alternatively examine the difference of GFRF and GIRF with 2- and 11-layer models. Based on the structural configuration in Figure 1, the building can be modeled as 11 layers, with the top 11th layer being the same as the 2nd layer in the 2-layer model, and with the first ten layers having the same total flight time as the first layer in the 2-layer model. Due to the story-to-story proximity in structure in Figure 1, the flight time for the first 10 layers is assumed to be equally shared with each of the ten layers in the 11-layer model. The minor difference in each of the first 10 story heights in Figure 1 then leads to slightly-different velocity in the first 10 layers and $r_{1\,j} \cong 1$ for *j*=1~10. This yields Eq. 3b to

$$T_{jj^-} \cong T_{j^-j} \cong 1\,, \quad R_{jj^-} \cong R_{j^-j} \cong 0 \qquad \text{(22a b)}$$

and with the fact of zero *R*s in inter-

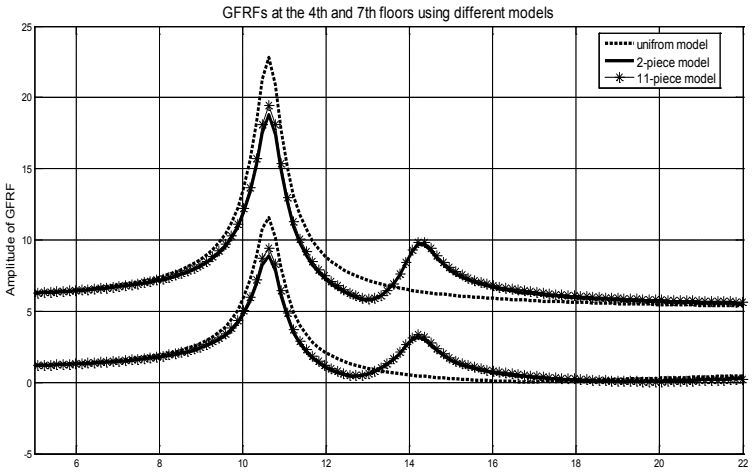

Figure 7. Comparison of GFRF amplitudes at the 4th and 7th floors with respect to impulsive basement motion obtained with 1-layer, 2-layer and 11-layer mod*els* from seismic recordings and models

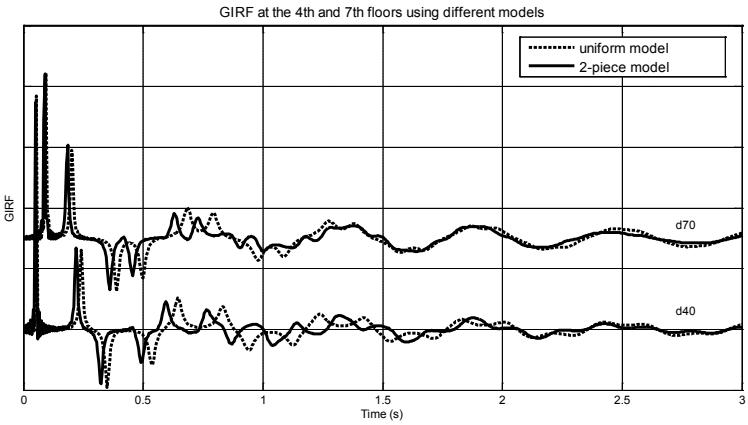

Figure 8. Comparison of GIRFs at the 4th and 7th floor with respect to impulsive basement motion obtained with 1- and 2-layer models

stories shown in Eq. 3a, Eq. 5 can be simplified as

$$T_{ln} \cong T_{lm}T_{mn}\ ,\ R_{ln} = R_{mn}\ ,\ \ for\ \ l,m,n = 1 \sim 10 \tag{23}$$

Subsequently, this leads to the *T*s and *R*s in the first ten layers in the 11-layer model similar to those with the first layer in the 2-layer model. With those *Ts* and *R*s, GFRF with the 11-layer model obtained from Eq. 2a with *N*=11 is essentially similar to Eqs. 6a,b with the 2-layer model.

With parameters used in Table 1, Figure 7 shows that both the 2-layer and 11-layer models are consistent to each other in GFRF, in addition to capturing the two modal frequencies. On the other hand, wave and vibration features in GFRF and GIRF with 1-layer uniform model is qualitatively different from those in the 2- and/or 11-layer models, in which the former model cannot capture the motions with the second modal frequency, as shown in Figure 7. The difference can also be seen in Figure 8, although it is not as qualitatively clear as in Figure 7.

In summary, the presented analysis suggests that the 2-layer model is effective in system identification for buildings structures like the Millikan Library in general, and in improved accuracy in capturing high-order (2nd in this example) wave motions in particular. The increased number of layers in the modeling is not essentially helpful in capturing fundamental low-order wave features for the building with relatively-uniform floors/stories along the height. It could, nevertheless, be useful in system identification and damage detection with strong non-uniform structure in height.

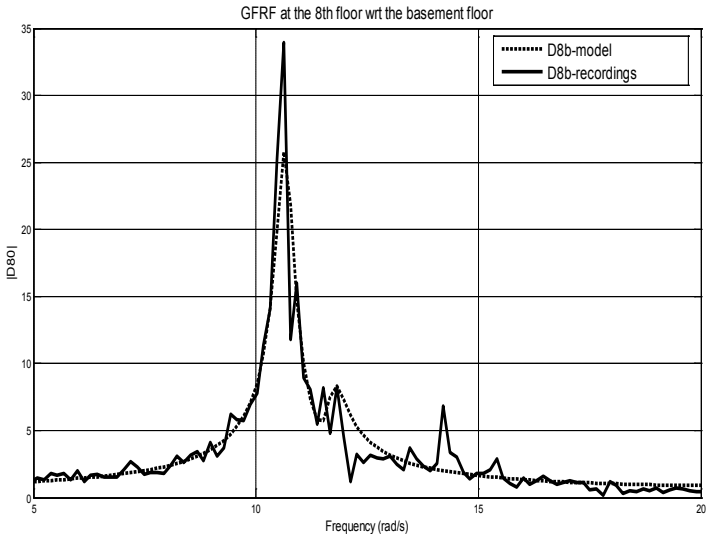

Figure 9. System identification using seismic recordings at the basement and 8th floor with continuous-discrete model matching two modal frequencies at 10.62 and 11.67 rad/s

Parametric Identification with Continuous-Discrete Model

In general, the more the number of DOF used for a building system, the more robust the system identification is. This sub-section shows some results of the system identification using the continuous-discrete model with seismic recordings provided at the basement and 8th floor. The identification algorithm is carried out in frequency range 5~22 *rad/s* by numerically minimizing the mean squared difference of recording- and model-based GFRF with match at two pairs of identified modal frequencies, i.e., (10.62, 11.67) rad/s for one case and (10.62, 14.21) rad/s for the other, while it is assumed to use the same floor mass in the first 10 floors (corresponding to the basement up to the 9th floor in Figure 1) and massless in the roof, the same wave speed in the first 10 inter-stories, pre-selected damping ratios, and true inter-story height in Figure 1.

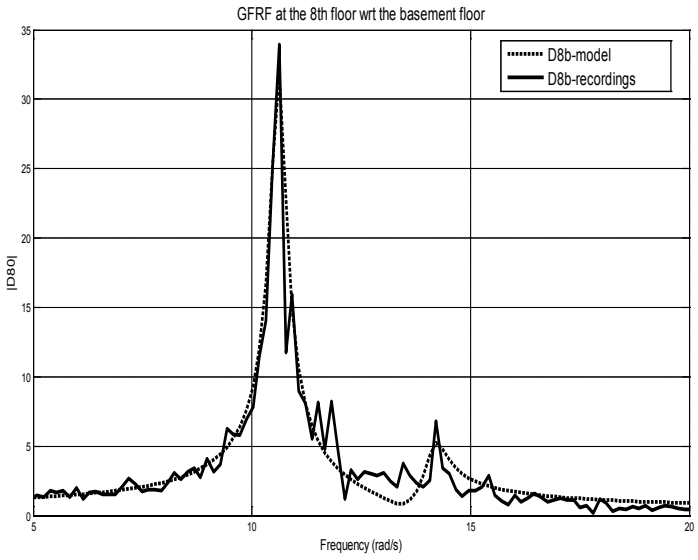

Figure 9b: System identification using seismic recordings at the basement and 8th floor with continuous-discrete model matching two modal frequencies at 10.62 and 14.21 rad/s

Figures 9a,b show the match between recording- and model-based GFRF at modal frequencies (10.62, 11.67) and (10.62, 14.21) rad/s respectively, from which the identified model parameters are summarized in the Table 1. These results

show that continuous-discrete modeling could flexibly capture dominant dynamic features of the system, exemplified as any two (or more in principle) modal frequencies identified from seismic recordings. In contrast, the 2-layer model cannot identify the reasonable building parameters with the pre-selected modal frequencies (10.62, 11.67) rad/s. The identified floor-to-story mass ratio, playing a major role in determining the other parameters, is also consistent with the realistic calculation based on design configuration of floors, columns and shear walls.

It should also be pointed out that this case identification builds on pre-selections and pre-assumptions of some system parameters with only a pair of seismic recordings available, aiming to show the robustness of the wave-based approach with limited number of recordings in comparison with traditional vibration-based discrete one. As the number of available recordings becomes large enough exemplified as 11 sets for this case, both traditional MDOF and presented continuous-discrete models make less and possibly negligible difference in system identification.

Table 1. Identified system parameters pertinent to different models and earthquake recordings

Earthquake/ Model		ω_1 *(rad/s)*	ω_2 *(rad/s)*	v *(m/s)*	γ	Others
Lytle EQ (Chopra, 1995)		12.08	52.36	-	0.029	-
San Fernando EQ (Chopra, 1995)		10.13	48.33	-	0.064	-
Yorba Linda EQ September 3, 2002	One-layer model (Snider and Safak, 2006)	10.77	-	322	0.024	H=48.2m
	One-layer model (Zhang et al., 2011)	10.62	-	326	0.028	H= 48.2m
	2-layer model	10.62	14.21	v_1=361.85 v_2=19.18	γ_1=0.03 γ_2=0.03	h_1=45.77m, h_2=2.43m
	11-layer model	10.62	14.21	$v_j=h_j$/0.0136 *(j=1-10)* v_{11}=19.18	γ_j=0.03 *(j=1-11)*	h_j (j=1-9) from one mid-story to the next Figure 1; h_{11}=2.43 m
	Case 1: 11-floor-story model	10.62	11.67	v_j=430 (j=1~10) v_{11}=29	γ_j=0.025, γ_{fj}=0.025, (j=1~10)	h_j (j=1-10) same as Figure 1, r_{mj}=0.44 (j=1~10), r_{m11}=0
	Case 2: 11-floor-story model	10.62	14.21	v_j=345 (j=1~10) v_{11}=27.8	γ_j=0.020, γ_{fj} =0.030, (j=1~10)	h_j (j=1-10) same as Figure 1, r_{mj}=0.40 (j=1~10), r_{m11}=0

CONCLUSIONS

This study presents an in-depth understanding for seismic motion in shear-deformation building with a continuous-discrete model and degenerated ones. It then applies the model and its various degenerated ones for system identification of Millikan Library building with a pair of recordings of Yorba Linda earthquake of September 3, 2002. Results show the wave-based approach with continuous-discrete modeling is efficient and robust in comparison with the traditional vibration-based ones.

ACKNOWLEDGMENTS

This work was supported by the Colorado School of Mines – Petroleum Institute joint research project under the auspices of Abu Dhabi National Oil Company. The opinions, findings and conclusions expressed herein are those of the authors and do not necessarily reflect the views of the sponsors.

REFERENCES

Banerjee, S., Ricci, F., Monaco, E. and Mal, A. (2009). "A wave propagation and vibration-based approach for damage identification in structural components", *Journal of Sound and Vibration,* 322, 167–183.

Beyen, K. (2008). "Structural identification for post-earthquake safety analysis of the Fatih mosque after the 17 August 1999 Kocaeli earthquake", *Engineering Structures*, 30, 2165–2184.

Cai, G.Q. and Lin, Y.K. (1991). "Localization of wave propagation in disordered periodic structures", *AIAA Journal*, 29(3), 450–456.

Chopra, A. (1995). *Dynamics of structures- theory and applications to earthquake engineering*, Prentice-Hall, Inc.

Gargab, L.O. (2012). *Continuum modeling and identification of high-rise buildings using seismic recordings*, *PhD Thesis*, Colorado School of Mines, Golden, Colorado, USA.

Hong, A., Betti1, L.R. and Lin, C.C. (2009). "Identification of dynamic models of a building structure using multiple earthquake records", *Struct. Control Health Monit.,* 16. 178–199.

Iwan, W.D. (1996). "Drift spectrum: measure of demand for earthquake ground motions", *Journal of Engineering Mechanics-ASCE*, 123, 397-404.

Kawakami, H. and Oyunchimeg, M. (2003). "Normalized input-output minimization analysis of wave propagation in buildings", *Engineering Structures*, 25(11), 1429-1442.

Kawakami, H. and Oyunchimeg, M. (2004). "Wave propagation modeling analysis of earthquake records for buildings", *Journal of Asian Architecture and Building Engineering*, 3(1), 33-40.

Kohler, M.D., Heaton, T. and Bradford, S.C. (2007). "Propagating Waves in the Steel Moment-frame Factor Building Recorded During Earthquakes", *Bull. Seism. Soc Am.*, 97(4), 1334-1345.

Lin, Y.K. and Cai, G.Q. (1995). *Probabilistic structural dynamics-advanced theory and applications*, McGraw-Hill,Inc.

Lin Y.K. and Wu, W.F. (1984). "A closed form earthquake response analysis of multistory building on compliance soil", *Journal of Structural Engineering*, 12(1), 87-110.

Oyunchimeg, M. and Kawakami, H. (2003). "A new method for propagation analysis of earthquake waves in damaged buildings: Evolutionary normalized input-output minimization (NIOM)", *Journal of Asian Architecture and Building Engineering*, 2(1), 9-16.

Safak, E. (1999). "Wave Propagation Formulation of Seismic Response of Multistory Building", *Journal of Structural Engineering ASCE,* 125(4), 426-437.

Snieder, R. and Safak, E. (2006). "Extracting the Building Response Using Siesmic Interferometery: Theory and Application to The Millikan Library in Pasadena, California", *Bull. Seism. Soc. Am.* 96(2), 586-598.

Snieder, R., Sheiman, J. and Calvert, R. (2006). "Equivalence of virtual-source method and wave-field deconvolution in seismic interferometry", *Physical Review*, E73:066620 (9 pages)

Todorovska, M.I. (2009a). "Seismic interferometry of a soil-structure interaction model with coupled horizontal and rocking response", *Bull. Seism. Soc. Am.*, 99(2A), 611-625.

Todorovska, M.I. (2009b). "Soil-structure system identification of Millikan Library North-South response during four earthquake (1970-2002): what caused the observed wandering of the system frequencies?", *Bull. Seism. Soc. Am.*, 99(2A), 626-635.

Todorovska, M.I., Ivanovic, S.S. and Trifunac, M.D. (2001). "Wave Propagation in a Seven-story Reinforced Concrete Building I: Theoritical Models", *Soil Dynamics and Earthquake Engineering*, 21, 211-223.

Uluso, H.S., Feng, M.Q. and Fanning, P.J. (2011). "System identification of a building from multiple seismic records", *Earthquake Engng Struct. Dyn.* 40, 661–674.

Xu, Y.L., Chen, S.W. and Zhang, R. (2003). "Modal identification of Di Wang building under typhoon York using HHT method", *Structural Design of Tall and Special Buildings,* 12, 21-47.

Zhang, R. (2000). "Some observations on modeling of wave motion in a layer-based elastic medium", *Journal of Sound and Vibration*, 229(5), 1193–1212.

Zhang, R., Al Hilali, S., Abdulla, A. and Al Kurbi, M. (2010). "A Wave-based Approach for Seismic Response Analyses of High-Rise Buildings", *Proceedings of the IUTAM Symposium*, Vol. 29, *Nonlinear Stochastic Dynamics and Control* (Zhu, Lin and Cai, eds.), 336-346, ISBN: 978-94-007-0731-3.

Zhang, R., Snieder, R., Gargab, L. and Seibi, A. (2011). "Modeling of seismic wave motion in high-rise buildings", *Probabilistic Engineering Mechanics*, 26, 520–527.